Excited State Competition in *fac*-[Re^{I}(dppz)(CO)$_3$(py-PTZ)]$^+$

W. Doug Bates, Pingyun Chen, Dana M. Dattelbaum, Wayne E. Jones, Jr., and Thomas J. Meyer*

Department of Chemistry, The University of North Carolina at Chapel Hill,
Chapel Hill, North Carolina 27599-3290

Received: February 15, 1999; In Final Form: April 25, 1999

Following Re^I → dppz (dppz is dipyrido[3,2-*a*:2′,3′-*c*]phenazine) metal-to-ligand charge transfer (MLCT) excitation of *fac*-[Re(dppz)(CO)$_3$(py-PTZ)]$^+$ (py-PTZ is 10-(4-picolyl)phenothiazine), there is a dynamic competition between intramolecular electron and energy transfer. Laser flash photolysis at 420 nm in 1,2-dichloroethane produces the MLCT excited state *fac*-[Re^{II}(dppz$^{\cdot-}$)(CO)$_3$(py-PTZ)]$^{+*}$. It undergoes intramolecular energy transfer to give the dppz-localized $\pi\pi^*$ excited state [Re^I(^{3}dppz)*(CO)$_3$(py-PTZ)]$^+$ ($^3\pi\pi^*$) in competition with electron transfer to give the redox-separated state (RS) [Re^I(dppz$^{\cdot-}$)(CO)$_3$(py-PTZ$^{\cdot+}$)]$^+$. The $\pi\pi^*$ state decays to the ground state with $k = 1.7 \times 10^4$ s^{-1} ($\tau = 60 \pm 15$ μs) and the RS state decays with $k = 9.1 \times 10^6$ s^{-1} ($\tau = 110 \pm 10$ ns). The competition ratio for formation of the two is [RS]/[$^3\pi\pi^*$] ∼ 2.4. Subsequent $^3\pi\pi^*$ → RS interconversion is slow even though the process is favored by 0.43 eV.

Introduction

There is an extensive chemistry of chromophore−quencher (C−Q) complexes in which electron or energy transfer donors and/or acceptors are covalently linked to metal-to-ligand charge transfer (MLCT) chromophores.[1−11] An example is *fac*-[Re^I(bpy)(CO)$_3$(py-PTZ)]$^+$ (bpy is 2,2′-bipyridine and py-PTZ is 10-(4-picolyl)phenothiazine) in which Re^I → bpy MLCT excitation is followed by −PTZ → Re^{II} intramolecular electron transfer as shown in Scheme 1.[8] With both donors and acceptors present, these complexes begin to mimic some of the functional elements of the reaction center of photosynthesis.[12] C−Q complexes have also proven to be extremely valuable in the study of intramolecular electron and energy transfer.[11]

In an earlier paper, we demonstrated competitive quenching of the Re^{II}-Mebpy$^{\cdot-}$ MLCT excited state of *fac*-[Re^I(Mebpy-CH$_2$OCH$_2$An)(CO)$_3$(MQ$^+$)]$^{2+}$ (Mebpy-CH$_2$OCH$_2$An is 4-[(9-anthrylmethoxy)methyl]-4′-methyl-2,2′-bipyridine, MQ$^+$ is *N*-methyl-4,4′-bipyridinium) by energy and electron transfer. Energy transfer occurs to give *fac*-[Re^I[Mebpy-CH$_2$OCH$_2$-(^{3}An*)](CO)$_3$(MQ$^+$)]$^{2+}$. It is in competition with electron transfer to give *fac*-[Re^{II}(Mebpy-CH$_2$OCH$_2$An)(CO)$_3$(MQ$^\cdot$)]$^{2+*}$.[13]

In this manuscript, we explore a second competition, in this case between electron and energy transfer in *fac*-[Re^I(dppz)(CO)$_3$(py-PTZ)]$^+$ (**1**, dppz is dipyrido[3,2-*a*:2′,3′-*c*]phenazine). Ligand structures are illustrated below.

Experimental Section

Materials. Spectroscopic measurements were performed in high purity solvents purchased from Burdick & Jackson. The supporting electrolyte [N(*n*-C$_4$H$_9$)$_4$](PF$_6$), TBAH, was purchased from Aldrich, recrystallized from hot ethanol twice, and dried in a vacuum oven at 80 °C for 72 h.

Preparations. The preparation of the dppz ligand was described elsewhere.[14−16]

SCHEME 1: In CH$_3$CN at 295 K

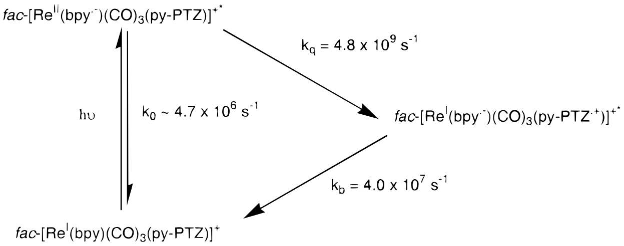

fac-[Re^I(dppz)(CO)$_3$Cl]. To a solution of 90.8 mg (0.251 mmol, 1.0 equiv) of Re(CO)$_5$Cl in 12 mL of toluene was added

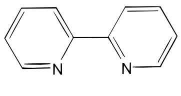

(bpy)

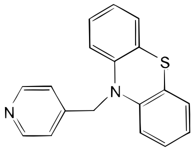

(py-PTZ)

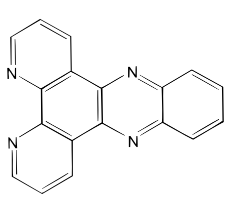

(dppz)

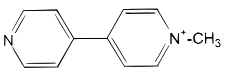

(MQ$^+$)

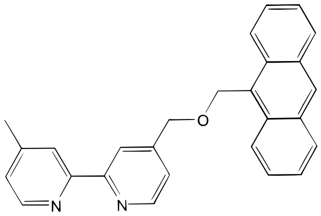

(Mebpy-CH$_2$OCH$_2$An)

---

* To whom correspondence should be addressed.

10.1021/jp990543z CCC: $18.00

85 mg (0.355 mmol, 1.2 equiv) of dppz. The stirred solution was heated at reflux under argon for 2.5 h. Upon cooling the solution to 0° C, a yellow precipitate appeared and was isolated by suction filtration. It was washed several times with cold Et_2O, and dried in vacuo to yield 120 mg (0.204 mmol, 81.4% yield). The product was used without further purification. Elemental analysis: Calculated for $ReC_{21}H_{10}ClN_4O_3$: C, 42.9; H, 1.71; N, 9.53. Found: C, 43.8; H, 2.20; N, 9.34. ^1H NMR (CD_2Cl_2): 9.85 (2H; dd, J = 1.5 and 7.9 Hz; H_1, H_8); 9.40 (2H; dd, J = 1.5 and 4.8 Hz; H_3, H_6); 8.44 (2H; dd, J = 3.4 and 5.6 Hz; H_{10}, H_{13}); 8.04 (2H; dd, J = 3.4 and 5.6 Hz; H_{11}, H_{12}); 8.02 (2H; dd, J = 4.8 and 7.9 Hz; H_2, H_7).

fac-[Re^I(dppz)(CO)$_3$(OTf)]. (OTf^- is trifluoromethanesulfonate anion.) To a solution of 125.5 mg (0.213 mmol, 1.0 equiv) of *fac*-[Re^I(dppz)(CO)$_3$Cl] in dry tetrahydrofuran (THF) was added 62 mg of AgOTf (0.239 mmol, 1.18 equiv). The solution was heated at reflux under argon for 2.5 h. The precipitated AgCl was filtered off and THF removed by rotary evaporation to yield a yellow oil. It was redissolved in CH_2Cl_2 and slowly added to an excess of cold, swirling pentane to precipitate the desired yellow-green salt. The salt was collected by suction filtration and washed with copious amounts of Et_2O to yield 0.143 g of product (0.203 mmol, 95.3%) which was used as an intermediate without further purification.

fac-[Re^I(dppz)(CO)$_3$(py-PTZ)](PF$_6$). To a stirring solution of 53 mg (0.075 mmol, 1 equiv) of *fac*-[Re^I(dppz)(CO)$_3$(OTf)] in 12 mL of degassed methanol was added 41.6 mg of py-PTZ (0.143 mmol, 1.9 equiv). The mixture was heated to reflux with stirring for 2.5 h under argon in the dark. Seven milliliters of aqueous saturated NH_4PF_6 was added and the solution was cooled to 0° C. The desired salt precipitated and was collected via suction filtration and washed with cold Et_2O. It was purified twice by redissolving in a minimal amount of CH_2Cl_2 and precipitated by adding into swirling cold isooctane. The precipitate was chromatographed on alumina with 2:1 CH_3CN/toluene to yield 29 mg of product (0.03 mmol, 40% yield). Elemental analysis: Calculated for $ReC_{39}H_{24}F_6N_6O_3PS$: C, 47.42; H, 2.45; N, 8.51. Found: C, 46.76; H, 2.73; N, 8.47. ^1H NMR (CD_2Cl_2): 9.98 (2H; dd, J = 1.3 and 8.2 Hz; H_1, H_8); 9.58 (2H; dd, J = 1.2 and 5.2 Hz; H_3, H_6); 8.48 (2H; dd, J = 1.3 and 8.2 Hz; H_{10}, H_{13}); 8.27 (2H; dd, J = 5.3 and 8.3 Hz; H_2, H_7); 8.19 (2H; d, J = 6.7 Hz; *2,6-py*-CH_2−PTZ); 8.105 (2H; dd, J = 3.4 and 6.6 Hz; H_9 and H_{12}); 7.31 (2H; d, J = 6.7 Hz; *3,5-py*-CH_2−PTZ); 7.05 (2H; dd, J = 1.35 and 7.35 Hz; py-CH_2-*PTZ-1,9*); 6.83 (4H; ddd, J = 1.2, 6.6 and 8.0 Hz; py-CH_2-*PTZ-2,3,7,8*); 6.41 (2H; d, J = 8.1 Hz; py-CH_2-*PTZ-4,6*); and 4.94 (2H; s; py-CH_2−PTZ).

Purification. Metal complex salts were purified by cation-exchange HPLC on a Brownlee CX-100 Prep 10 column by utilizing a 4 mM KBr, CH_3CN/KH_2PO_4 (pH = 7.0) buffered linear gradient controlled by a Perkin-Elmer Series 4 pump control unit and monitored with a Perkin-Elmer LC-95 variable UV−vis spectrophotometer detector fitted with a 4.5 μL flow cell. Metathesis of the resulting Br^- salt to the corresponding PF_6^- salt was achieved by addition of saturated aqueous NH_4PF_6 followed by slow removal of CH_3CN, causing precipitation of the desired product. To ensure complete metathesis, salts were redissolved in a minimal amount of CH_3CN, an equal volume of saturated aqueous NH_4PF_6 was added, and CH_3CN was slowly removed. The PF_6^- salts were collected on glass frits, washed with copious amounts of Et_2O, and thoroughly dried in vacuo. Complexes purified in this manner were analyzed for contaminants by analytical HPLC in the same manner as described above.

Measurements. UV−vis spectra were recorded either on an HP8452A spectrophotometer in 1-cm quartz cuvettes with a solvent-subtracted background or on a Cary 14 upgraded by On-Line-Instrument Systems in matching 1-cm quartz cells. Cyclic voltammograms were measured by using a Princeton Applied Research model 173 potentiostat. Electrochemical experiments were performed in one compartment cells with 0.1 M TBAH as the supporting electrolyte in spectrograde CH_3CN. The working and counter electrodes were a Pt bead and Pt coil, respectively. All potentials were recorded versus a saturated sodium calomel electrode (SSCE) and were uncorrected for junction potentials. Solutions were deaerated by purging with Ar or N_2 for at least 5 min prior to cycling. $E_{1/2}$ values are reported as an average of cathodic and anodic peaks with $\Delta E_p \sim 60-90$ mV for most couples unless otherwise noted.

Samples for emission and excitation experiments were prepared as optically dilute solutions (ca. 10^{-5} M) in CH_3CN or 1,2-dichloroethane (DCE) and freeze−pump−thaw degassed for a minimum of four cycles (ca. 10^{-6} Torr), then sealed under vacuum. Measurements at 77 K were made with a liquid N_2 quartz finger Dewar (made from nonemissive Supracil quartz) and 8 mm diameter glass sample cells.

Continuous wave (CW) emission spectra were obtained with a SPEX Fluorolog F212-A photon-counting spectrofluorimeter equipped with either Hamamatsu R636 red sensitive or Hamamatsu R928 photomultiplier tubes (PMT). Optical response characteristics for the Spex Fluorolog and PMT detectors were corrected with a calibration curve generated with 1.0 mm slits by using a National Institute of Standards and Technology (NIST) calibrated 250 W tungsten lamp (Optronics Laboratories, Inc., model 220M), controlled by a precision current source at 6.50 W (Optronics Laboratories, Inc., model 65). No corrections for self-absorption were made; overlap between absorption and emission spectra was insignificant. Relative emission quantum yields, ϕ_{em}, were measured in optically dilute solutions employing *fac*-[Re^I(bpy)(CO)$_3$(4-Etpy)]$^+$ (ϕ_{em} = 0.18 in CH_3CN) as a standard.[17]

Emission lifetimes were obtained with instrumentation described earlier.[18] Emission decay profiles were acquired by employing a PRA LN 1000/LN 102 nitrogen laser/dye laser combination for exciting the sample. Emission was monitored at 90° to the excitation source by using a PRA B204−3 monochromator and a cooled, 10-stage, Hamamatsu R928 PMT coupled to either a LeCroy 9400 digital oscilloscope or a LeCroy 6880/6010 transient digitizer interfaced to an IBM PC. The absorbance of the sample was ∼0.1 at the excitation wavelength.

Transient absorption measurements were conducted with a system described elsewhere.[19] The experiments used either the third harmonic of a Nd:YAG laser (λ_{ex} = 354.7 nm) or the third harmonic was coupled to a PDL-2 pulsed dye laser to produce 420 nm pulses for excitation (∼3 mJ/pulse). The excitation beam was at a right angle to an Applied Photophysics laser kinetic spectrometer. The spectrometer consisted of a 250 W pulsed Xe arc probe source, *f*/3.4 grating monochromator, and a five-stage PMT. The output was collected by using either a LeCroy 9400 digital oscilloscope or a LeCroy 6880/6010 transient digitizer interfaced to an IBM PC. Electronic control and synchronization of the laser, probe, and digitizer were provided by electronics of our own design. Samples were prepared as described for emission experiments at a concentration of $\sim 5 \times 10^{-5}$ M. To avoid sample degradation, a cell was employed that allowed for replacement of the solution after the acquisition of three data points (∼60 shots). Decay rate constants evaluated by single wavelength kinetics were calculated by analysis of

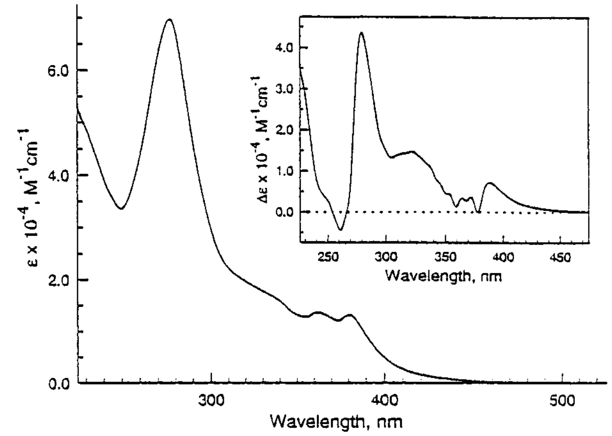

Figure 1. UV−vis absorption spectrum of *fac*-[Re^I(dppz)(CO)$_3$(py-PTZ)]$^+$ in CH$_3$CN at 298 K with the inset showing the difference spectrum between *fac*- [Re^I(dppz)(CO)$_3$(py-PTZ)]$^+$ and dppz.

the average of 20 decay traces. Lifetimes by transient absorption measurements were calculated by least-squares analysis of plots of ln(I/I_0) vs time where I and I_0 are the transmitted intensities at times t and 0, respectively.

Results

The absorption spectrum of *fac*-[Re^I(dppz)(CO)$_3$(py-PTZ)]$^+$ (**1**) in CH$_3$CN is shown in Figure 1 and the structure of the complex is illustrated below.

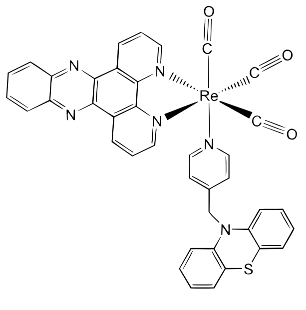

1

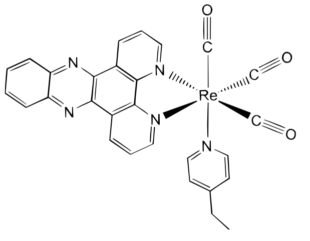

2

On the low energy side of the absorption manifold, there are bands arising from overlapping MLCT and $\pi \rightarrow \pi^*$ transitions. The presence of the latter is shown by the appearance of vibronic components at 362 and 380 nm. The difference spectrum between the C−Q complex and free dppz is shown in the inset in Figure 1.

Emission from **1** displays vibronic structure typical of emission from a $\pi\pi^*$state, but the emission quantum yield (ϕ_{em} = 0.0036) is less than that for the model complex, *fac*-[Re^I-(dppz)(CO)$_3$(4-Etpy)]$^+$(**2**, ϕ_{em} = 0.0244) which is known to be a $^3\pi\pi^*$(dppz) emitter.[14,20,21] In cyclic voltammograms of **1** in CH$_3$CN (0.1 M TBAH vs SSCE), reversible waves appear for reduction of dppz (at $E_{1/2}$ = −0.89 V), oxidation of PTZ (at 0.84 V), and irreversible oxidation of Re^I to Re^{II} at $E_{p,a}$ = +1.60 V.

In Figure 2A are shown transient absorption difference spectra for **1** acquired in DCE at a series of times following laser flash excitation at 420 nm. For comparison, the difference spectrum for **2** acquired 1000 ns after the laser pulse is shown in Figure 2B. Transient IR measurements were used to demonstrate that the lowest excited state in **2** is a $^3\pi\pi^*$ state.[14,20] The absorption feature at $\lambda_{max} \sim$ 470 nm arises from a $\pi^* \rightarrow \pi^*$ transition in $^3\pi\pi^*$(dppz). It decays with τ = 40 μs (k = 2.5 × 10^4 s^{-1}) in DCE at 298 K. The same 470 nm absorption feature appears in the transient spectrum of **1**. Decay kinetics in this case, Figure 2A, are nonexponential and wavelength-dependent. The absor-

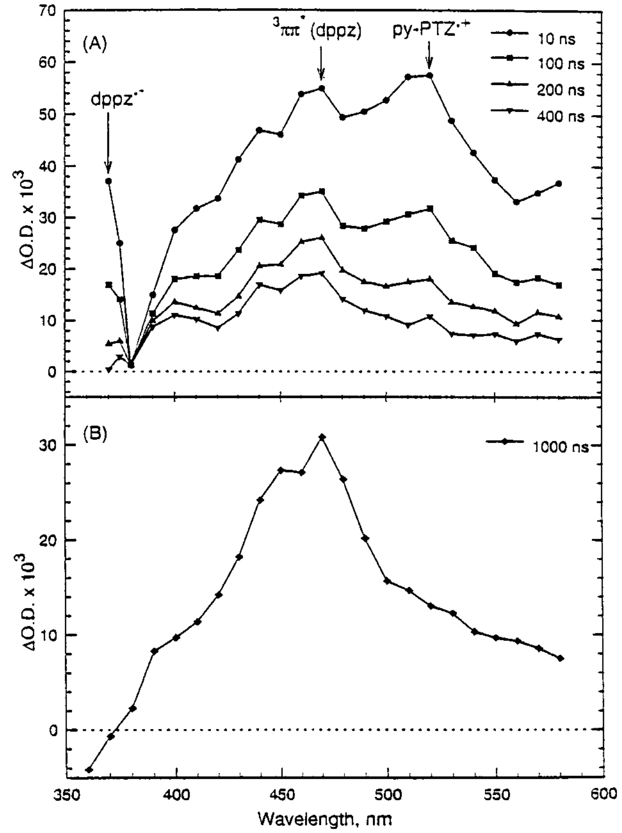

Figure 2. Transient absorption difference spectra for *fac*-[Re^I(dppz)-(CO)$_3$(py-PTZ)]$^+$(A) obtained at various times and *fac*-[Re^I(dppz)(CO)$_3$-(4-Etpy)]$^+$(B) obtained 1000 ns after the laser pulse in DCE at 298 K. Excitation at 420 nm, 3 mJ/pulse.

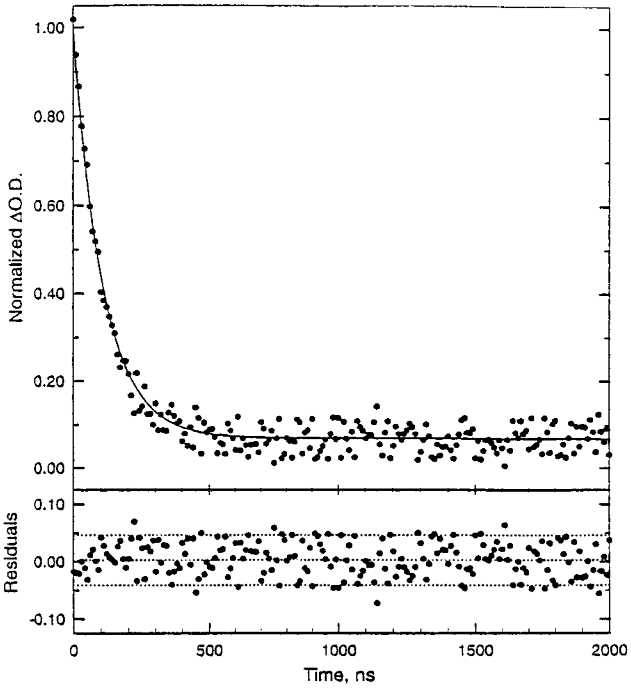

Figure 3. Fit of transient absorption decay for the fast process in *fac*-[Re^I(dppz)(CO)$_3$(py-PTZ)]$^+$ in DCE at 298 K to first-order kinetics with k = 9.1 × 10^6 s^{-1}(τ = 110 ± 10 ns) with excitation at 420 nm (3 mJ/pulse) and monitoring at 500 nm.

SCHEME 2: In DCE at 298 K

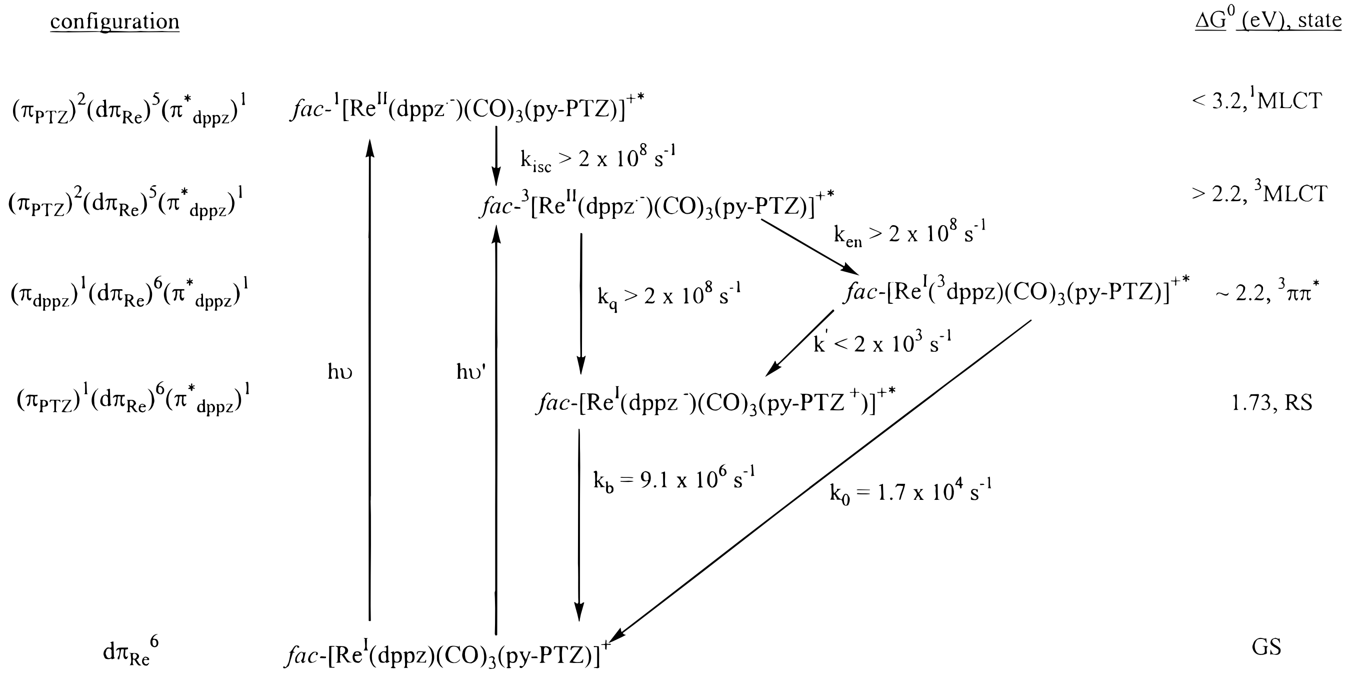

bance−time transients can be fit to two components. One decays rapidly and concomitantly with the loss of the PTZ$^{·+}$ absorption at 520 nm. The second decays slowly with the loss of the $^3\pi\pi^*$(dppz) absorption at 470 nm. A fit of the decay data for the faster process to the exponential function, $A - A_\infty$ (= ΔO.D.) = ($A_0 - A_\infty$) exp(-kt), with A, A_0, and A_∞ the absorbances at times t, 0, and 1 μs at 500 nm, respectively, is shown in Figure 3, with $k_1 = 9.1 \times 10^6$ s^{-1} (τ_1 = 110 ± 10 ns). Decay kinetics for the slower process were also first order with $k_2 = 1.7 \times 10^4$s^{-1} (τ_2 = 60 ± 15 μs).

Discussion

From the absorption spectrum in Figure 1, absorption by fac-[Re^I(dppz)(CO)$_3$(py-PTZ)]$^+$ at the exciting wavelength of 420 nm is dominated by Re^I → dppz MLCT excitation. Compared to the model, **2**, $^3\pi\pi^*$(dppz) emission is partly quenched and both −PTZ$^{·+}$ and $^3\pi\pi^*$(dppz) appear as products as shown by the transient absorption features at ~510 and ~470 nm, respectively. They form during the ~5 ns laser pulse and decay on different time scales.

The photophysical properties of **1** can be accounted for by the sequence of reactions in Scheme 2. Re^I → dppz excitation at 420 nm is largely MCLT in character producing fac-[Re^{II}(dppz$^{·-}$)(CO)$_3$(py-PTZ)]$^{+*}$. Absorption is dominated by transitions which give MLCT states largely singlet in character (^{1}MLCT) and emission by a closely spaced manifold of states which are largely triplet (^{3}MLCT).[22] Based on the lowest energy feature in the difference spectrum in the inset in Figure 1, the energy of ^{1}MLCT is < 3.2 eV. There is some contribution to the absorption spectrum on the low energy side from bands arising from direct excitation to ^{3}MLCT with the absorption gaining intensity by spin−orbit coupling-induced mixing of singlet and triplet states by the $d\pi^5$(Re^{II}) core. The spin−orbit coupling constant for Re^{II} is 2900 cm^{-1}.[22] The conversion from singlet to triplet states (k_{isc} in Scheme 2) is presumably rapid (<100 fs in [Ru(bpy)$_3$]$^{2+}$)[23] and the MLCT triplets are the states in which the competition occurs.

The competition is between internal conversion to give $^3\pi\pi^*$(dppz), by the transition $(\pi_{dppz})^2(d\pi_{Re})^5(\pi^*_{dppz})^1 \rightarrow (\pi_{dppz})^1(d\pi_{Re})^6(\pi^*_{dppz})^1$, and electron transfer to give the redox-separated (RS) state fac-[Re^I(dppz$^{·-}$)(CO)$_3$(py-PTZ$^{·+}$)]$^+$, by $(\pi_{PTZ})^2(d\pi_{Re})^5(\pi^*_{dppz})^1 \rightarrow (\pi_{PTZ})^1(d\pi_{Re})^6(\pi^*_{dppz})^1$. The energy of $^3\pi\pi^*$(dppz) is ≤ 2.2 eV on the basis of the highest energy vibronic component in the emission spectra of **1** and **2**. It is 1.73 eV for the RS state from the difference between $E_{1/2}$ values for the PTZ$^{+/0}$ and dppz$^{0/+}$ couples by cyclic voltammetry.

Schematic energy diagrams for the three states along a coupled, averaged solvent coordinate are shown in Figure 4. The transition ^{3}MLCT → $^3\pi\pi^*$(dppz) is nonadiabatic and interconverts different excited states of the same Hamiltonian. It is a vibronic transition induced by vibrational coupling and the matrix element,

$$V_k = \hbar\left(\frac{\hbar\omega_k}{2\mu_k}\right)^{1/2} \langle\psi'|^{\partial}/_{\partial Q_k}|\psi\rangle \tag{1}$$

In this equation, μ_k, ω_k, and Q_k are the reduced mass, angular frequency, and normal coordinate, respectively, of a vibration of appropriate symmetry to mix the electronic states, the promoting mode. ψ' and ψ are the final and initial electronic wave functions. This transition is largely spin-allowed because the final state is a dppz triplet and the initial state is largely triplet with some singlet character mixed in by spin−orbit coupling.

The transition, ^{3}MLCT → RS, is an electron-transfer reaction between π_{PTZ} and $d\pi_{Re}$ orbitals which are weakly coupled electronically given the intervening −CH$_2$- bridge. The electron-transfer matrix element interconverting these states is of the form

$$H_{DA} = \langle\psi'|\hat{H}|\psi\rangle \tag{2}$$

in which $\hat{H}$ is an electrostatic operator. In this transition, the largely triplet character of the MLCT excited state should also be transferred to the products with the triplet component, ^{3}RS, greatly in excess of the singlet, ^{1}RS. Writing the wave functions ψ' and ψ as the product of electronic, ψ_{el}, and spin wave

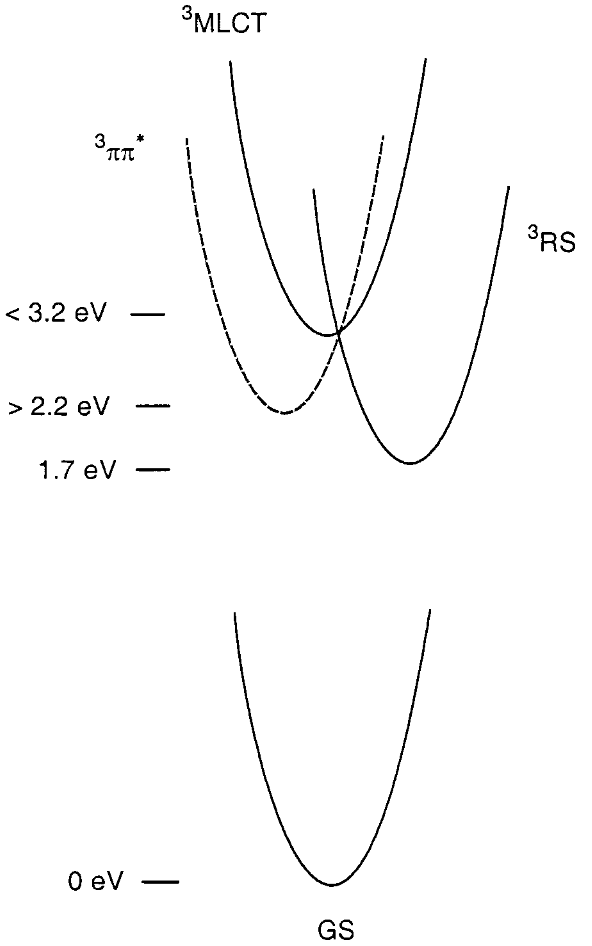

Figure 4. Schematic energy diagram along a coupled solvent coordinate illustrating the relative energies of $^3\pi\pi^*$, ^{3}RS, and ^{3}MLCT.

functions, ψ_s, the spin wave function for ^{3}MLCT can be written as

$$\psi_s = {}^3\phi + \alpha{}^1\phi \qquad (3)$$

with the ground state a spin singlet.

In eq 3, $^3\phi$ and $^1\phi$ are the pure triplet and singlet wave functions and α is the mixing coefficient of $^1\phi$ in ψ_s. The rate constant for the ^{3}MLCT → RS transition varies with $H_{DA}{}^2$, and the fractional composition of singlet products in the RS state is α^2. Even with α as high as 0.2, only 4% of the RS states formed would be singlets.

The relative amounts of $^3\pi\pi^*$(dppz) and RS in the competition can be estimated from the transient absorption spectral changes in Figure 2 and Beer's law by using known molar extinction coefficients: For $^3\pi\pi^*$(dppz), $\epsilon_{470} = 15\,000$ M^{-1}cm^{-1} and $\epsilon_{510} = 7000$ M^{-1}cm^{-1},[24] and for $-$PTZ$^{\cdot+}$, $\epsilon_{470} = 3760$ M^{-1}cm^{-1} and $\epsilon_{510} = 7490$ M^{-1} cm^{-1}.[8] On the basis of these values and the ΔO.D. changes, the competition ratio is [RS]/[$^3\pi\pi^*$] $\sim$2.4. This analysis reveals that the $\pi\pi^*$ state is the minor product in the competition. This is consistent with the fact that $\pi\pi^*$ emission from **1** is considerably decreased compared to that from **2**. The competition ratio is a direct measure of the relative rate constants for intramolecular electron transfer (k_q in Scheme 2) and energy transfer (k_{en}) with $k_q/k_{en} \sim 2.4$. In a previous study, it was shown that $-$PTZ → Re^{II} electron transfer in *fac*-[Re^{II}(bpy$^{\cdot-}$)(CO)$_3$(py-PTZ)]$^{+*}$ is rapid with $k = 4.8 \times 10^9$ s^{-1}, $\tau = 0.21$ ns in CH$_3$CN at 295 K.[8]

The lifetime of the $\pi\pi^*$(dppz) state in **1** (60 μs) is slightly longer than the $\pi\pi^*$(dppz) state in **2** (40 μs) and there is no evidence for the reaction $^3\pi\pi^*$(dppz) → ^{3}RS. This is an electron-transfer reaction in which the change in electronic configuration is $(\pi_{dppz})^1(\pi_{PTZ})^2(d\pi_{Re})^6(\pi^*_{dppz})^1 \xrightarrow{k'} (\pi_{dppz})^2(\pi_{PTZ})^1(d\pi_{Re})^6(\pi^*_{dppz})^1$. It is favored by $\sim$0.5 eV but is slow, at least on the 60 μs time scale for decay of $^3\pi\pi^*$(dppz), and $k' < 2 \times 10^3$ s^{-1}. As illustrated in Figure 4, this is presumably a reaction in the normal region. Factors that contribute to slow electron transfer in this region are a large classical solvent barrier and weak $\pi_{PTZ}-\pi_{dppz}$ electronic coupling through the $-$CH$_2$-bridge.

Acknowledgment. We acknowledge financial support from the National Science Foundation under Grant CHE-9705724.

References and Notes

(1) Balzani, V.; Scandola, F. *Supramolecular Photochemistry*; Ellis Horwood: New York, 1991.
(2) Collin, J.-P.; Guillerez, S.; Sauvage, J.-P.; Barigelletti, F.; Flamigni, L.; De Cola, L.; Balzani, V. *Coord. Chem. Rev.* **1991**, *111*, 291.
(3) Furue, M.; Yoshidzumi, T.; Kinoshita, S.; Kushida, T.; Nozakura, S.; Kamachi, M. *Bull. Chem. Soc. Jpn.* **1991**, *64*, 4.
(4) Ryu, C. K.; Wang, R.; Schmehl, R. H.; Ferrere, S.; Ludwikow, M.; Merkert, J. W.; Headford, C. E. L.; Elliot, C. M. *J. Am. Chem. Soc.* **1992**, *114*, 430.
(5) Schanze, K. S.; MacQueen, D. B.; Perkins, T. A.; Cabana, L. A. *Coord. Chem. Rev.* **1993**, *122*, 63.
(6) Westmoreland, T. D.; Le Bozec, H.; Murray, R. W.; Meyer, T. J. *J. Am. Chem. Soc.* **1983**, *105*, 5.
(7) Westmoreland, T. D.; Schanze, K. S.; Neveux, J. P. E.; Danielson, E.; Sullivan, B. P.; Chen, P.; Meyer, T. J. *Inorg. Chem.* **1985**, *24*, 2596.
(8) Chen, P. Y.; Westmoreland, T. D.; Danielson, E.; Schanze, K. S.; Anthon, D.; Neveux, P. E.; Meyer, T. J. *Inorg. Chem.* **1987**, *26*, 1116.
(9) Danielson, K.; Elliott, C. M.; Merkert, J. W.; Meyer, T. J. *J. Am. Chem. Soc.* **1987**, *109*, 2519.
(10) Balzani, V.; Juris, A.; Venturi, M.; Campagna, S.; Serroni, S. *Chem. Rev.* **1996**, *96*, 759.
(11) Schanze, K. S.; Walters, K. A. Photoinduced Electron Transfer in Metal-Organic Dyads. Ramanurthy, V., In *Molecular and Supramolecular Photochemistry*; Schanze, K. S., Eds.; Marcel Dekker: New York, 1998; Vol. 2.
(12) Gust, D.; Moore, T. A. *Science* **1989**, *244*, 35−41.
(13) Mecklenburg, S. L.; Opperman, K. A.; Chen, P.; Meyer, T. J. *J. Phys. Chem.* **1996**, *100*, 15145−15151.
(14) Bates, W. D. Ph.D. Dissertation, University of North Carolina at Chapel Hill, Chapel Hill, NC, 1995.
(15) Summers, et al. *Aust. J. Chem.* **1970**, *23*, 1023.
(16) Amougal, et al. *J. Chem. Soc. Trans.* **1990**, 1841.
(17) Worl, L. A.; Duesing, R.; Chen, P.; Della Ciana, L.; Meyer, T. J. *J. Chem. Soc., Dalton Trans.* **1991**, 849−858.
(18) Tapolsky, G.; Duesing, R.; Meyer, T. J. *Inorg. Chem.* **1990**, *29*, 2285−2297.
(19) Chen, P.; Danielson, E.; Meyer, T. J. *J. Phys. Chem.* **1988**, *92*, 3708−3711.
(20) Schoonover, J. R.; Bates, W. D.; Meyer, T. J. *Inorg. Chem.* **1995**, *34*, 6421.
(21) Schoonover, J. R.; Strouse, G. F.; Dyer, R. B.; Bates, W. D.; Chen, P.; Meyer, T. J. *Inorg. Chem.* **1996**, *35*, 273−274.
(22) Striplin, D. R.; Crosby, G. A. *Chem. Phys. Lett.* **1994**, *221*, 426−430.
(23) Damrauer, N. H.; Cerullo, G.; Yeh, A.; Boussie, T. R.; Shank, C. V.; McCusker, J. K. *Science* **1997**, *275*, 54−57.
(24) Del Barrio, J. I.; Rebato, J. R.; G.-Tablas, R. M. *J. Mol. Spectrosc.* **1988**, *132*, 238.